Nonlinear output response of acousto-optic modulated distributed Bragg reflector (DBR) fiber laser

MAN-HONG LAI[a], MD RAJIBUL ISLAM[a,*], KOK-SING LIM[a,b], SHIRLEY DIONG-CHEA FANG[b], HANG-ZHOU YANG[c], XUEGUANG QIAO[c], HARITH AHMAD[a,b]
[a]*Photonics Research Centre, University of Malaya, 50603 Kuala Lumpur, Malaysia*
[b]*Department of Physics, Faculty of Science, University of Malaya, 50603 Kuala Lumpur, Malaysia*
[c]*College of Physics, Northwest University, Xi'an, Shaanxi 710069, China*

This article presents a study on the output response of a distributed Bragg reflector (DBR) to acousto-optic wave. In the fabrication, the DBR is constructed with a 12 cm long EDF and two FBGs that share the same center wavelength. The behavior of the DBR under the influence of acousto-optic wave can be well explained based on the model of a single sinusoidal-modulated FBG. A nonlinear response has been observed for DBR output amplitude which is similar to the reflectivity variation at the center wavelength of an FBG impinged by acousto-optic wave. The potential for using DBR as a vibration sensor has been investigated in the frequency range of 120 kHz-190 kHz.

(Received December 20, 2014; accepted September 29, 2016)

Keywords: Distributed Bragg reflector (DBR), Acousto-optic wave, FBG, Vibration sensing

1. Introduction

Fiber Bragg grating laser based sensors have been attracted considerable interests due to its advantages of compact size, inherent self-referencing capability, multiplexing capability and higher signal-to-noise ratio. Distributed Bragg reflectors (DBR) are one of the admired fiber lasers for sensing applications. DBR is fabricated by developing a resonator using two Bragg gratings that share the same Bragg wavelength and a gain medium of erbium doped fiber as the fiber cavity between them. Excellent performance makes it a distinguished technique for small linewidth and high optical signal to noise ratio (OSNR) laser generation. DBR shares the similar characteristics like FBG and it is responsive to various measurands such as temperature, refractive index, pressure, bending, vibration and etc. [1-3]. Besides, it is insensitive to Bragg wavelength and it does not require a tunable laser source to match the specific wavelength of the gratings. Conspicuously, the usual responses of DBRs to strain have been well-studied [4] and these are prospective sensors for several applications including structural health monitoring, machinery fault detection, online monitoring for cracks or leakage in undersea oil wells, pipelines, etc. The leak signature in pressured pipeline or enclose cavity can be detected from the generated acoustic emission mostly in the ultrasonic region where the ambient background noise is very low [5]. Generally, a linear response of the DBR sensor to acoustic vibration is considered during the application of DBR sensor [6]. However, the second harmonic generation is observed at higher acoustic vibration amplitude. This effect distorts the signal received by the DBR, which reduced its accuracy in vibration detection.

In this paper we have proposed an approach to form the DBR fiber laser. Both theoretical and experimental analysis have been carried out to evaluate the output response of a DBR fiber laser acoustically modulated using Piezo-Transducer (PZT). An exciting phenomenal consequence has been found over a certain range of frequency and power density of the vibration signal. To validate our experimental outcome we have visualized a simulated result of acousto-optic modulated DBR fiber laser response. The output power is modulated by acoustic pressure and narrow linewidth of the output of DBR laser offers much higher detection sensitivity. The amplitude of acoustic wave can be determined by measuring the frequency of the laser output using a comparatively low-cost photodetector and a commercial optical spectrum analyzer (OSA). The advantages of this technique are inexpensive and simple.

2. Structure of DBR fiber laser

DBR is constructed with two FBGs and a short segment of Erbium-doped fiber (EDF). To attain a high throughput DBR, FBGs with sufficiently high reflectivity and matched Bragg wavelengths are used so that the emitted power from the EDF can oscillate between two reflective gratings. The reflective bandwidth of the FBGs and the cavity length are the keys to controlling the number of longitudinal modes within the resonator and output laser stability. Although shorter laser cavity

promises better laser stability but it produces lower throughput power. A remedy to this trade-off is by reducing the reflective bandwidth of one of the gratings. This can be achieved by adopting uniform grating structure which is known for its small bandwidth for both FBGs in the DBR.

In the FBG fabrication, SMF-28 fibers are first soaked in a hydrogen gas tank at a pressure of 1700 psi for 7 days to enhance their UV photosensitivity. After that, the grating inscription is performed using 248 nm KrF excimer laser and phase mask. To achieve uniform grating, the laser beam size is expanded from ~6 mm to ~45 mm using a beam expander and then the tails of the Gaussian laser beam are removed using a vertical slit to attain a beam with uniform intensity. For better observation and control of the grating reflectivity, wavelength and reflection bandwidth, in-situ monitoring on the FBG transmission spectrum is performed during the UV writing process to ensure the desired specifications are achieved. The fabricated FBGs are then annealed at 90°C for 4 hours to accelerate out-diffusion of the residue hydrogen gas in the fiber and stabilize the Bragg wavelengths and reflectivity.

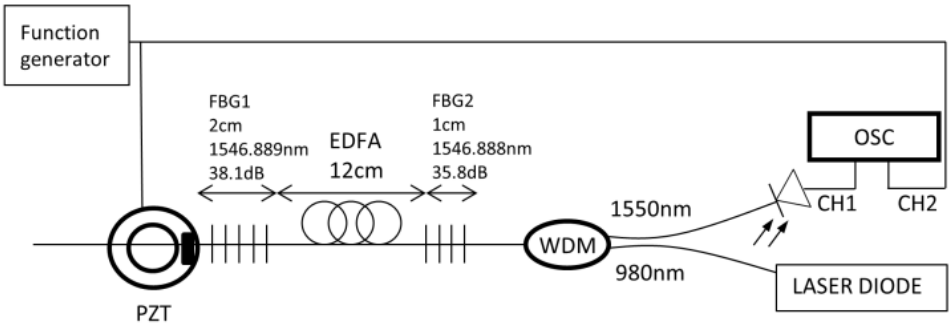

Fig. 1. Schematic diagram of experimental setup (WDM: wavelength-division multiplexer coupler; PZT: piezoelectric transducer; EDF: Erbium – doped fiber; OSC: digital oscilloscope)

More than 20 FBGs are produced and all of them are carefully characterized to seek for the best two FBGs with the matched Bragg wavelength, small bandwidths and high reflectivity for the construction of DBR. The EDF used is L-band_fiber (DF1500l) manufactured by Fiber core Ltd. The DBR is constructed by fusion splicing two wavelength matched FBGs to the both ends of the EDF. Fig. 1 shows the experimental setup for the manufactured DBR. The employed FBGs share the similar Bragg wavelength at ~1546.889 nm and have a negligible wavelength difference of 0.001nm. FBG2 that has a shorter grating length, a reflectivity (35.8dB) and a bandwidth of 0.21nm is placed at the position closer to the WDM coupler while the other FBG (FBG1) that has higher reflectivity (38.1dB) and larger bandwidth (0.254 nm) is placed at the position further away from the WDM coupler.

This is a commonly used configuration to enable higher output laser emission through the FBG that has lower reflectivity. The role of the WDM coupler besides coupling pump laser source to the DBR, it collects throughput laser from the DBR to the photodetector where the optical signal is converted into electrical signal and subsequently analyzed and recorded using a digital oscilloscope. Both PZT and FBG1 are placed on a same aluminum plate and spaced 1cm apart. The generated acoustic wave is transferred to the DBR sensor through the aluminum place and the signal is given by the function generator. The EDF has a length of 12cm and the acoustic wave influence on FBG2 is smaller after the attenuation along the fiber. In addition to that, the sensitivity of the shorter grating (FBG2) is lower therefore it is fair to assume that such configuration complies the aforementioned conditions of the theoretical model that only FBG1 is subjected to the influence of acoustic wave and the DBR output response is similar to the FBG. The laser performance of the DBR is as depicted in Fig. 2. At pump power of 420mW, the throughput power is -12dBm. The rollover of the curve is due to the thermal effects induced by the pump laser. The absorption of pump light in the active fiber leads to asymmetric heating in the laser cavity, which causes the reflection spectra of the FBGs to shift with respect to each other. This cause large fluctuations in the output power of the DBR laser as well [7].

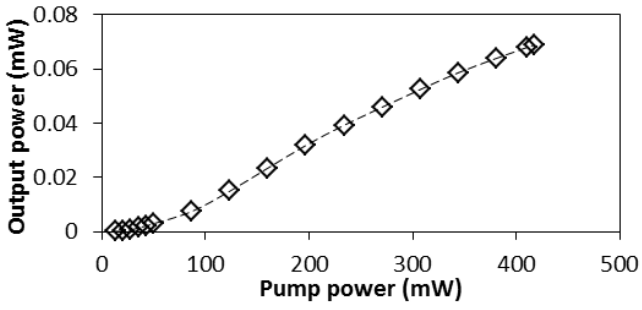

Fig. 2. The output performance of the DBR with increasing pump power

3. Theoretical analysis of DBR fiber laser response to acoustic wave

In the field of acoustic and ultrasonic wave, the pressure of acoustic and ultrasound wave modify the glass refractive index of the fiber due to the photo elastic effect. Change in refractive index is given by [8]

$$\frac{\Delta n}{n} = \frac{n^2 \Delta P}{2E}(1-2\nu)(2\rho_{12}+\rho_{11}) \tag{1}$$

$$\Delta n = \frac{n^3 \Delta P}{2E}(1-2\nu)(2\rho_{12}+\rho_{11}) \tag{2}$$

where ν is Poisson's ratio , ρ_{11} and ρ_{12} are the fiber strain tensor components. For an acoustic wavelength comparable with or much smaller than the fiber grating length, the acoustic pressure induces different index changes and, therefore, changes the physical length and grating periods. Change in physical length and grating period is given by

$$\frac{\Delta L}{L} = \frac{\Delta \Lambda}{\Lambda} = \frac{(1-2\nu)\Delta P}{E} \tag{3}$$

where E is Young's modulus of the glass fiber.

The time dependent function of the acoustic pressure wave is given by [9]

$$\Delta P(z,t) = \Delta P_0 \cos(\frac{2\pi}{\lambda_a} - \omega t) \tag{4}$$

where λ_a is the acoustic wavelength.

The modified dc-component of the coupling coefficient for the perturbed grating is given by

$$\sigma(z,t) = \frac{2\pi}{\lambda}(\delta n + \Delta n) \tag{5}$$

δn is the index modulation amplitude of the grating.

The ac-component of coupling coefficient is un-perturbed which is given by used

$$\kappa = \frac{\nu \pi \delta n}{\lambda} \tag{6}$$

Detuning δ can be expressed as

$$\delta(z,t) = \frac{2\pi n_{eff}}{\lambda} - \frac{\pi}{\Lambda_0 + \Delta\Lambda} \tag{7}$$

The output spectrum can be simulated using Transfer Matrix Method (TMM) where each local section of the FBG is described by a matrix F

$$F = \begin{pmatrix} \cosh(\gamma_B \Delta z) - i\frac{\hat{\sigma}}{\gamma_B}\sinh(\gamma_B \Delta z) & -i\frac{\kappa}{\gamma_B}\sinh(\gamma_B \Delta z) \\ i\frac{\kappa}{\gamma_B}\sinh(\gamma_B \Delta z) & \cosh(\gamma_B \Delta z) + i\frac{\hat{\sigma}}{\gamma_B}\sinh(\gamma_B \Delta z) \end{pmatrix} \tag{8}$$

where $\gamma_B = \left[\kappa^2 - \hat{\sigma}^2(z)\right]^{1/2}$ and $\hat{\sigma}(z) = \delta(z) + \sigma(z)$ is a general dc self-coupling coefficient. Acoustic wave modulates the refractive index along the grating of FBG and this information has been incorporated in transfer matrix method in the simulation. TMM described in [10] is used to produce the result.

4. Results and discussion

Fig. 3 illustrates the simulated reflection spectra of a 2 cm long uniform FBG impinged by an acousto-optic wave. The dotted curves denote the reflection spectra at different phase condition of π and –π from the reference (solid curve). The DBR laser is generated at the center wavelength, λ_{center} of the FBG, the wavelength position where the reflectivity is maximum. Since the other FBG is far away from the source and it is out of zone of influence, the output response of the DBR is similar to that of a single FBG. Upon the perturbation of acoustic wave pressure along the grating, the output response of the DBR can be determined from the variation of reflectivity at the center wavelength as illustrated in the inset in Fig. 3.

As a result, the reflection curve is oscillating around λ_{center} and the laser output is modulated according to variation of reflectivity at λ_{center}. Considering the fact that the reflection curve at center wavelength (DBR laser wavelength) is nonlinear, a distorted output response is produced.

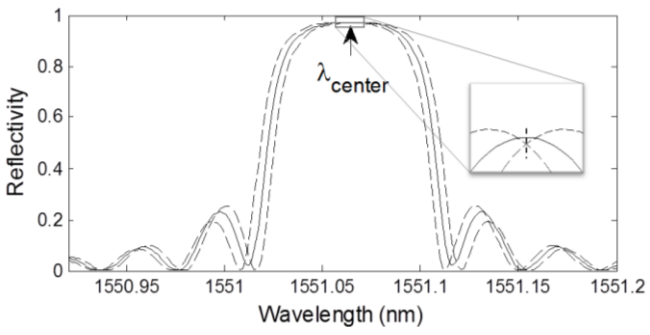

Fig. 3. Simulated reflection spectra of a 2cm uniform FBG impinged with 150 kHz flexural vibration (acoustic wavelength = 3.5cm). The dashed curves are the results of impinged acoustic wave with a phase difference of π and –π from that of solid curve

Figs. 4 (a) and (b) present the simulation and experimental result of the DBR acoustic optically modulated at 150 kHz, within the vicinity of the resonant frequency of the PZT. A distortion is observed in the output response of the DBR and both results are in excellent agreement. The distortion is growing with increasing impinging acoustic pressure. The magnitude of distortion can be interpreted from the amplitude of the second harmonic as presented in Fig. 5(a). The harmonic has a frequency twice as much as the incident/input acoustic wave frequency. At high input amplitude, the generated second harmonic amplitude is higher and may supersede the amplitude of fundamental frequency. Besides 150 kHz, the frequency response of the DBR in the range of 120 kHz-190 kHz is investigated (see Fig. 5(b)). We observed similar frequency responses but with different magnitudes of distortion due to the frequency dependent vibration strength (voltage-displacement response) of the PZT. The highest second harmonic (~20% of the fundamental frequency amplitude) is observed at 140 kHz of acoustic vibration input, followed by 160 kHz (~18%) and 120 kHz (~17%). The lowest second harmonic is observed at 150, 170, and 180 kHz of acoustic vibration input, which is ~5% of the fundamental frequency amplitude.

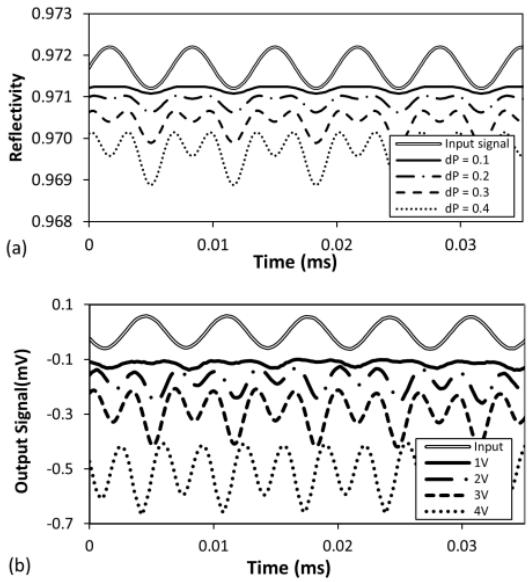

Fig. 4. Comparison between the (a) simulation and (b) experiment results. 'dP' is acoustic pressure in arbitrary unit, which is linearly proportional to the amplitude of acoustic wave

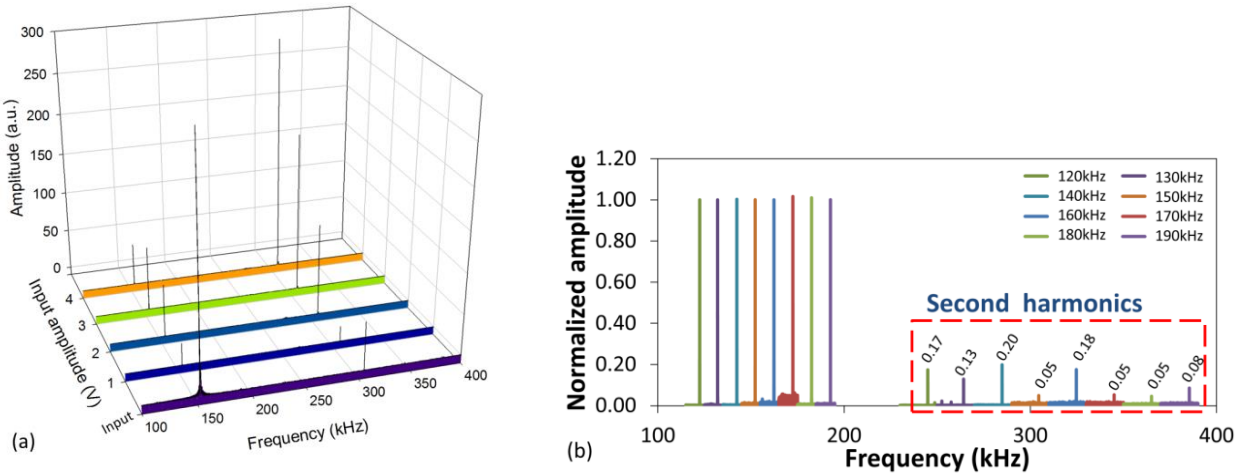

Fig. 5. Output frequency responses of the DBR for different (a) input amplitude and (b) frequency (120 kHz – 190 kHz)

5. Conclusion

We have proposed a new approach to form a DBR fiber laser for acousto-optic sensing. The proposed laser is theoretically and experimentally investigated its properties under the influence of acoustic wave. Due to the nonlinear reflection curve of the FBG, distorted output signal is observed in the experiment and it is in excellent agreement with the simulated result based on transfer matrix method. Second harmonic component is produced as the result of distortion and it depends on the strength of the acoustic wave. This finding is important for understanding the acousto-optic behavior of DBR and this device pose a great potential for the applications in optical signal processing and vibration sensing.

Acknowledgements

We would like to acknowledge UMRG Grant (RP019-2012C) and FRGS (FP002-2013A) for funding this project. This work is also partially supported by the National Natural Science Foundation of China (Nos.

60727004, 61077060, 61205080, 61235005), National High Technology Research and Development Program 863(Nos. 2007AA03Z413, 2009AA06Z203), Ministry of Education Project of Science and Technology Innovation (No. Z08119), Ministry of Science and Technology Project of International Cooperation (No. 2008CR1063), Shaanxi Province Project of Science and Technology Innovation (Nos. 2009ZKC01-19, 2008ZDGC-14).

References

[1] Y. R. García, J. M. Corres, J. Goicoechea, Journal of Sensors **2010**, 1 (2010).
[2] H. S. Jang, K. N. Park, J. P. Kim, S. J. Sim, O. J. Kwon, Y.-G. Han, K. S. Lee, Opt. Express **17**, 3855 (2009).
[3] M. S. Ferreira, M. Becker, H. Bartelt, P. Mergo, J. L. Santos, O. Frazão, Laser Phys. Lett. **10**, 095102 (2013).
[4] H. Zhang, J. Luo, B. Liu, S. Wang, C. Jia, X. Ma, Microw. Opt. Technol. Lett. **51**, 2559 (2009).
[5] S. Tanaka, H. Somatomo, A. Wada, N. Takahashi, Proc. SPIE 7503, 20th International Conference on Optical Fiber Sensors, 75033C (October 05, 2009).
[6] B. O. Guan, H. Y. Tam, S. T. Lau, H. L. W. Chan, IEEE Photon. Technol. Lett. **16**, 169 (2005).
[7] Y. Z. Xu, H. Y. Tam, S. Y. Liu, M. S. Demokan, IEEE Photonics Technology Letters **10**, 1253 (1998).
[8] Y.-J. Rao, Measurement science and technology **8**, 355 (1997).
[9] D. C. Betz, G. Thursby, B. Culshaw, W. J. Staszewski, Smart Materials and Structures **12**, 122 (2003).
[10] T. Liu, M. Han, IEEE Sensors J. **12**, 2368 (2012).

*Corresponding author: md.rajibul.islam@gmail.com